Novel Cassette Assay To Quantify the Outer Membrane Permeability of Five β-Lactams Simultaneously in Carbapenem-Resistant *Klebsiella pneumoniae* and *Enterobacter cloacae*

Tae Hwan Kim,[a]* Xun Tao,[a] Bartolome Moya,[a] Yuanyuan Jiao,[a] Kari B. Basso,[b] Jieqiang Zhou,[a] Yinzhi Lang,[a] Dhruvitkumar S. Sutaria,[a] Alexandre P. Zavascki,[c] Afonso L. Barth,[c,d] Stephanie M. Reeve,[e] Herbert P. Schweizer,[f] Deanna Deveson Lucas,[g] John D. Boyce,[g] Robert A. Bonomo,[h,i,j] Richard E. Lee,[e] Beom Soo Shin,[k] Arnold Louie,[l] George L. Drusano,[l] Jürgen B. Bulitta[a]

[a]Departments of Pharmaceutics and Pharmacotherapy and Translational Research, College of Pharmacy, University of Florida, Orlando, Florida, USA
[b]Department of Chemistry, University of Florida, Gainesville, Florida, USA
[c]Universidade Federal do Rio Grande do Sul, Porto Alegre, Brazil
[d]Laboratório de Pesquisa em Resistência Bacteriana, Hospital de Clínicas de Porto Alegre, Porto Alegre, Brazil
[e]Department of Chemical Biology and Therapeutics, St Jude Children's Research Hospital, Memphis, Tennessee, USA
[f]Department of Molecular Genetics and Microbiology, Emerging Pathogens Institute, College of Medicine, University of Florida, Gainesville, Florida, USA
[g]Infection and Immunity Program, Monash Biomedicine Discovery Institute and Department of Microbiology, Monash University, Victoria, Australia
[h]Medical Service and GRECC, Louis Stokes Cleveland Department of Veterans Affairs Medical Center, Cleveland, Ohio, USA
[i]Departments of Medicine, Pharmacology, Molecular Biology and Microbiology, Biochemistry, and Proteomics and Bioinformatics, Case Western Reserve University School of Medicine, Cleveland, Ohio, USA
[j]CWRU–Cleveland VAMC Center for Antimicrobial Resistance and Epidemiology (Case VA CARES), Cleveland, Ohio, USA
[k]School of Pharmacy, Sungkyunkwan University, Suwon, Gyeonggi-do, South Korea
[l]Institute for Therapeutic Innovation, College of Medicine, University of Florida, Orlando, Florida, USA

Tae Hwan Kim and Xun Tao contributed equally to this article. Author sequence for this work was decided by coin toss.

ABSTRACT Poor penetration through the outer membrane (OM) of Gram-negative bacteria is a major barrier of antibiotic development. While β-lactam antibiotics are commonly used against *Klebsiella pneumoniae* and *Enterobacter cloacae*, there are limited data on OM permeability especially in *K. pneumoniae*. Here, we developed a novel cassette assay, which can simultaneously quantify the OM permeability to five β-lactams in carbapenem-resistant *K. pneumoniae* and *E. cloacae*. Both clinical isolates harbored a bla_{KPC-2} and several other β-lactamases. The OM permeability of each antibiotic was studied separately ("discrete assay") and simultaneously ("cassette assay") by determining the degradation of extracellular β-lactam concentrations via multiplex liquid chromatography-tandem mass spectrometry analyses. Our *K. pneumoniae* isolate was polymyxin resistant, whereas the *E. cloacae* was polymyxin susceptible. Imipenem penetrated the OM at least 7-fold faster than meropenem for both isolates. Imipenem penetrated *E. cloacae* at least 258-fold faster and *K. pneumoniae* 150-fold faster compared to aztreonam, cefepime, and ceftazidime. For our β-lactams, OM permeability was substantially higher in the *E. cloacae* compared to the *K. pneumoniae* isolate (except for aztreonam). This correlated with a higher OmpC porin production in *E. cloacae*, as determined by proteomics. The cassette and discrete assays showed comparable results, suggesting limited or no competition during influx through OM porins. This cassette assay allowed us, for the first time, to efficiently quantify the OM permeability of multiple β-lactams in carbapenem-resistant *K. pneumoniae* and *E. cloacae*. Characterizing the OM permeability presents a critical contribution to combating the antimicrobial resistance crisis and enables us to rationally optimize the use of β-lactam antibiotics.

IMPORTANCE Antimicrobial resistance is causing a global human health crisis and is affecting all antibiotic classes. While β-lactams have been commonly used against susceptible isolates of *Klebsiella pneumoniae* and *Enterobacter cloacae*, carbapenem-resistant isolates are spreading worldwide and pose substantial clinical challenges. Rapid penetration of β-lactams leads to high drug concentrations at their periplasmic target sites, allowing β-lactams to more completely inactivate their target receptors. Despite this, there are limited tangible data on the permeability of β-lactams through the outer membranes of many Gram-negative pathogens. This study presents a novel, cassette assay, which can simultaneously characterize the permeability of five β-lactams in multidrug-resistant clinical isolates. We show that carbapenems, and especially imipenem, penetrate the outer membrane of *K. pneumoniae* and *E. cloacae* substantially faster than noncarbapenem β-lactams. The ability to efficiently characterize the outer membrane permeability is critical to optimize the use of β-lactams and combat carbapenem-resistant isolates.

KEYWORDS *Enterobacter cloacae*, *Klebsiella pneumoniae*, LC-MS/MS, beta-lactams, carbapenem resistance, carbapenems, cassette assay, cephalosporins, monobactams, outer membrane, permeability, polymyxin resistance

Multidrug-resistant (MDR) Gram-negative bacteria are causing an urgent, global threat to human health (1). The outer membrane (OM) of Gram-negative species presents a formidable penetration barrier for antibiotics (2–4). Therefore, characterizing the rate of OM penetration is important to identify antibiotics that can reach high and effective target site concentrations (5). β-Lactams have been used for decades against susceptible isolates of *Klebsiella pneumoniae* and *Enterobacter cloacae* complex; however, their clinical utility has been compromised by the global rise of carbapenem-resistant (CR) isolates. More recently, many of these CR isolates have additionally gained resistance to polymyxins (6). To bind their bacterial target receptors in the periplasm, β-lactams have to penetrate the OM. However, there is limited tractable data on the rate of OM permeability for β-lactams in *K. pneumoniae* and many other Gram-negative species. More permeability data are available for *Escherichia coli* (7) and, to a lesser degree, *Pseudomonas aeruginosa* (8) and *E. cloacae* complex (9). For the latter pathogen, permeability data on carbapenems are lacking though.

β-Lactams are hydrophilic molecules, which penetrate the OM via one or multiple different porin channels. Once in the periplasm, β-lactams are subject to β-lactamase-mediated hydrolysis, the effect of efflux pump(s) (10), and covalent binding to their penicillin-binding protein (PBP) target receptors (11). The relative rates of these processes determine the target site concentration of β-lactams and ultimately the extent of inactivation of the PBPs (i.e., transpeptidases) in the periplasm. Simultaneous combinations of two β-lactams (i.e., double β-lactam therapy) have been evaluated with promising results in large clinical trials in the 1970s and 1980s (12). For such combinations, it is important to assess that both of the β-lactams can efficiently penetrate through OM porin(s) at the same time. To our knowledge, there are currently no data on a potential interaction of β-lactams during influx. Moreover, combination therapies using a β-lactam with a polymyxin or an aminoglycoside have been used to combat MDR isolates. The latter two antibiotics offer the possibility to permeabilize the OM toward the β-lactam as a mechanism of synergy (13–16). Overall, the ability to characterize the rate of OM penetration for β-lactams is critical for optimizing antibiotic monotherapies and combination therapies against MDR Gram-negative organisms.

To characterize permeability, cellular uptake assays have been used to quantify intracellular drug accumulation over time (17–20). These assays are not feasible for β-lactams in MDR Gram-negative species, since β-lactamases rapidly hydrolyze β-lactams in the periplasm. This very feature is, however, exploited by the Zimmermann-Rosselet penetration assay (7, 21), which assesses the decline of extracellular β-lactam concentrations due to β-lactamase-mediated hydrolysis in the periplasm. To date, this assay has been used with single β-lactams where the β-lactam

concentrations were quantified spectrophotometrically. This approach limits sensitivity and specificity and is not feasible for studying multiple β-lactams simultaneously. Assuming rapid hydrolysis in the periplasm, the extracellular concentration of rapidly penetrating β-lactams will decline faster than that of slowly penetrating β-lactams. The rate of OM penetration can then be estimated by comparing the rates of decline in intact and lysed bacteria. This presents a permeability-limited clearance scenario, which has been widely applied for studying uptake of metabolically unstable drugs into hepatocytes in the drug metabolism and pharmacokinetics area (22, 23).

Here, we aimed to develop the first liquid chromatography-tandem mass spectrometry (LC-MS/MS)-based assay, which can quantify the OM permeability of five β-lactams in MDR isolates simultaneously (i.e., a cassette assay). This assay was developed using carbapenemase (bla_{KPC-2})-producing clinical isolates of $K.$ $pneumoniae$ and $E.$ $cloacae$, which additionally carried other β-lactamases. Our $K.$ $pneumoniae$ isolate was polymyxin resistant (PB^r), whereas the $E.$ $cloacae$ isolate was polymyxin susceptible (PB^s); the latter isolate was identified as belonging to the species $E.$ $cloacae$. The presence of OM porins and β-lactamases was assessed via whole-genome sequencing and proteomics.

RESULTS

The polymyxin MICs were 64 mg/liter for the $K.$ $pneumoniae$ isolate (KP3800) and 0.5 mg/liter for the $E.$ $cloacae$ isolate (EC3800). The MICs for KP3800 and EC3800 were 128 and 4 mg/liter for imipenem, >256 and 4 mg/liter for meropenem, 128 and 16 mg/liter for cefepime, 64 and 16 mg/liter for ceftazidime, and >256 and 128 mg/liter for aztreonam, respectively.

Whole-genome sequencing. The KP3800 isolate belonged to $K.$ $pneumoniae$ MLST type 437 and harbored five β-lactamases; these included the bla_{KPC-2} (carbapenemase), bla_{TEM-1B} (extended-spectrum β-lactamase [ESBL]), $bla_{SHV-182}$ (ESBL, 99.88% sequence identity to reference), bla_{OXA-1} (class D β-lactamase), and $bla_{CTX-M-15}$ (ESBL). The EC3800 belonged to $E.$ $cloacae$ MLST type 270 and carried four β-lactamases, including the bla_{KPC-2} (carbapenemase), bla_{ACT-7} (AmpC β-lactamase, 95.2% sequence identity to reference), $bla_{CTX-M-8}$ (ESBL, 99.89% sequence identity to reference), and bla_{OXA-9} (class D β-lactamase).

Hydrolysis of β-lactams in lysed bacteria. We used freshly grown and lysed bacteria in late exponential growth phase at initial inocula of approximately 6.6×10^8 CFU/ml (average of replicates) for EC3800 and 1.6×10^8 CFU/ml for KP3800. The rate of hydrolysis was measured for five clinically relevant β-lactams over periods of up to 120 min. We studied two carbapenems (imipenem and meropenem), two cephalosporins (cefepime and ceftazidime), and aztreonam, all at initial drug concentrations ranging from 1 to 30 mg/liter. The average unbound plasma concentrations at steady-state expected at the highest clinical dose in critically ill patients ranged from approximately 8 to 38 mg/liter (see Table S1 in the supplemental material). With EUCAST MIC breakpoints for our five β-lactams ranging from 1 to 4 mg/liter, the studied concentrations of 1 to 30 mg/liter covered the clinically relevant range for each drug.

For lysed bacteria using both the discrete and cassette assay, imipenem and meropenem were hydrolyzed rapidly (Fig. 1 to 4, panels G and H). Cefepime and aztreonam were also hydrolyzed rapidly, but more slowly than the carbapenems (Fig. 1 to 4, panels I and J). In contrast, ceftazidime hydrolysis was slow in EC3800 and moderate in KP3800 (Fig. 1 to 4, panel K in all figures). The results from two additional replicates each for the cassette (Fig. S2 and S3) and discrete (Fig. S4 and S5) assays showed good reproducibility compared to the results from the first replicate (Fig. 1 to 4).

When β-lactams were directly exposed to β-lactamases of lysed bacteria, the estimated intrinsic hydrolysis clearance (CL$_{int}$; curve fits of individual data sets had an average r^2 of 0.973) was rapid for all β-lactams except ceftazidime. Overall, β-lactamase activity was significantly higher for KP3800 compared to EC3800 ($P < 0.01$, paired t test for the respective drugs). The CL$_{int}$ tended to be smaller for the cassette compared to that of the discrete assay, likely due to a small extent of drug-drug interaction at the
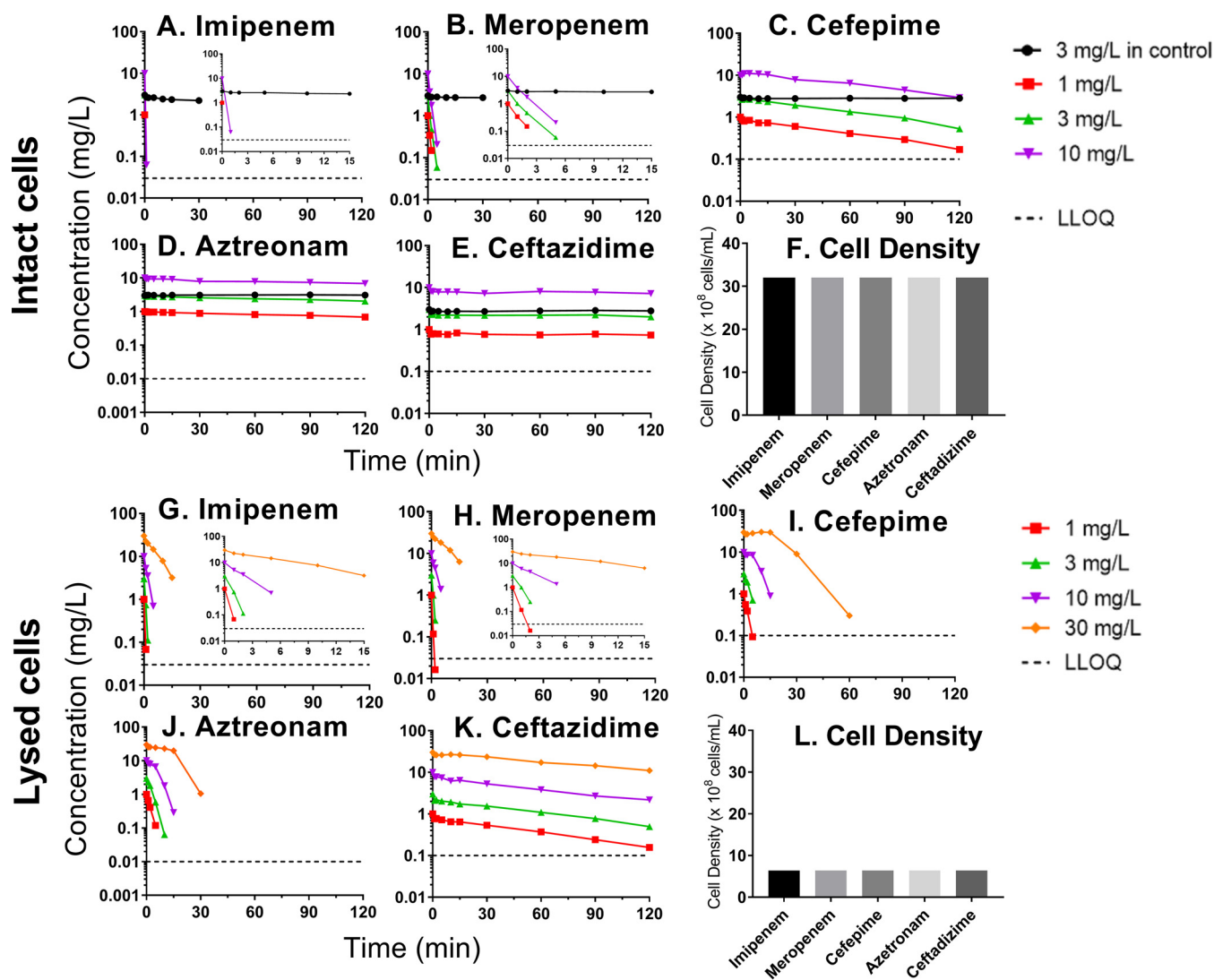
FIG 1 Concentration-time profiles of imipenem, meropenem, cefepime, ceftazidime, and aztreonam for the cassette assay of the polymyxin-susceptible *E. cloacae* isolate EC3800. β-Lactams were dosed at 3 mg/liter of each drug for the supernatant control and at 1, 3, or 10 mg/liter of each drug for intact bacteria arms (A to E). (F) Bacterial density (3.2 × 10⁹ cells/ml) after six washes and immediately before adding the antibiotics to the intact cell arms. β-Lactams were dosed at 1, 3, 10, or 30 mg/liter of each drug for lysed bacteria arms (G to K). (L) Bacterial density (6.4 × 10⁸ cells/ml) after the washes and immediately before lysing. The data (Table 1) represent biological triplicates. The individual profiles for all replicates are presented in the supplemental material.

β-lactamase during the cassette assay; however, the CL_{int} was still rapid for the cassette assay and the overall decline of β-lactam concentrations was permeability limited.

Depletion assay in the supernatant control and viability test. To improve sensitivity of the intact bacteria assay, we used high inocula of on average 3.3 × 10⁹ CFU/ml for EC3800 and 7.9 × 10⁸ CFU/ml for KP3800. This was achieved by concentrating bacteria from late-exponential-growth-phase cultures ~5-fold via centrifugation and resuspension. The five β-lactams were studied at initial concentrations of 1 to 10 mg/liter in intact bacteria. To demonstrate a lack of remaining β-lactamase activity after the sixth wash in phosphate-buffered saline (PBS), the β-lactam concentration was determined in the supernatant controls (i.e., "prior assay controls") using an initial concentration of 3 mg/liter. The β-lactam concentrations remained constant over 120 min for all five drugs in the prior assay controls under all conditions (i.e., for both isolates and for the discrete as well as the cassette assay, Fig. 1 to 4, panels A to E); this confirmed that extracellular β-lactamase activity was minimal after six washes.

To further demonstrate a lack of β-lactamase release into PBS during the intact bacteria assay, additional supernatant controls (i.e., "post assay controls") were studied;
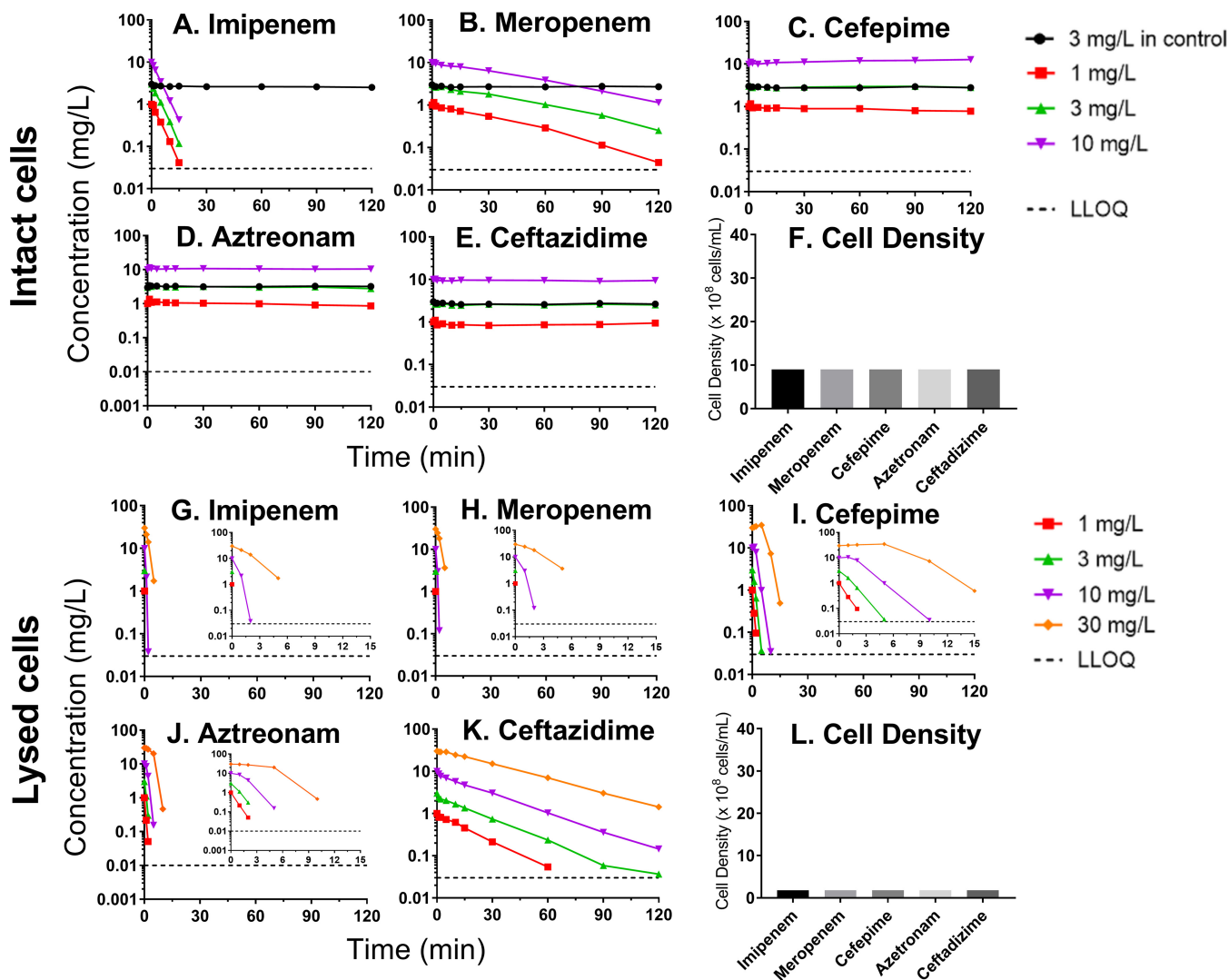
FIG 2 Concentration-time profiles of imipenem, meropenem, cefepime, ceftazidime, and aztreonam for the cassette assay of the polymyxin-resistant *K. pneumoniae* isolate KP3800. β-Lactams were dosed at 3 mg/liter of each drug for the supernatant control and at 1, 3, or 10 mg/liter of each drug for intact bacteria arms (A to E). (F) Bacterial density (9.0 × 10⁸ cells/ml) after six washes and immediately before adding the antibiotics to the intact cell arms. β-Lactams were dosed at 1, 3, 10, or 30 mg/liter of each drug for lysed bacteria arms (G to K). (L) Bacterial density (1.8 × 10⁸ cells/ml) after the washes and immediately before lysing. The data (Table 1) represent biological triplicates. The individual profiles for all replicates are presented in the supplemental material.

these controls used bacteria after six washes which had been further incubated in PBS for 120 min. After this incubation, bacteria were removed by centrifugation and the β-lactamase activity assessed in the supernatant. All five β-lactams were stable in the "post assay controls" (Fig. S1), confirming a lack of β-lactamase release during entire assay. In addition, we confirmed a lack of bacterial killing of EC3800 and KP3800 under simultaneous exposure to each of the five β-lactams at 10 mg/liter for 2 h in PBS buffer at a high initial bacterial density. There was no significant decline of viable counts for both EC3800 and KP3800 after 2 h of exposure to all five β-lactams, likely due to the high initial bacterial density and limited or no growth of bacteria in PBS buffer.

Depletion assay in intact bacteria. In intact EC3800, degradation of imipenem was extremely rapid and imipenem could only be quantified up to 1 min in the cassette study (Fig. 1 and 3, panels A). Imipenem was quantifiable up to 5 min in the discrete assay, since the bacterial density was ~5-fold lower than that in the cassette assay. Imipenem degradation remained relatively fast for intact KP3800 (Fig. 2 and 4, panels A) but was substantially slower than that for intact EC3800.
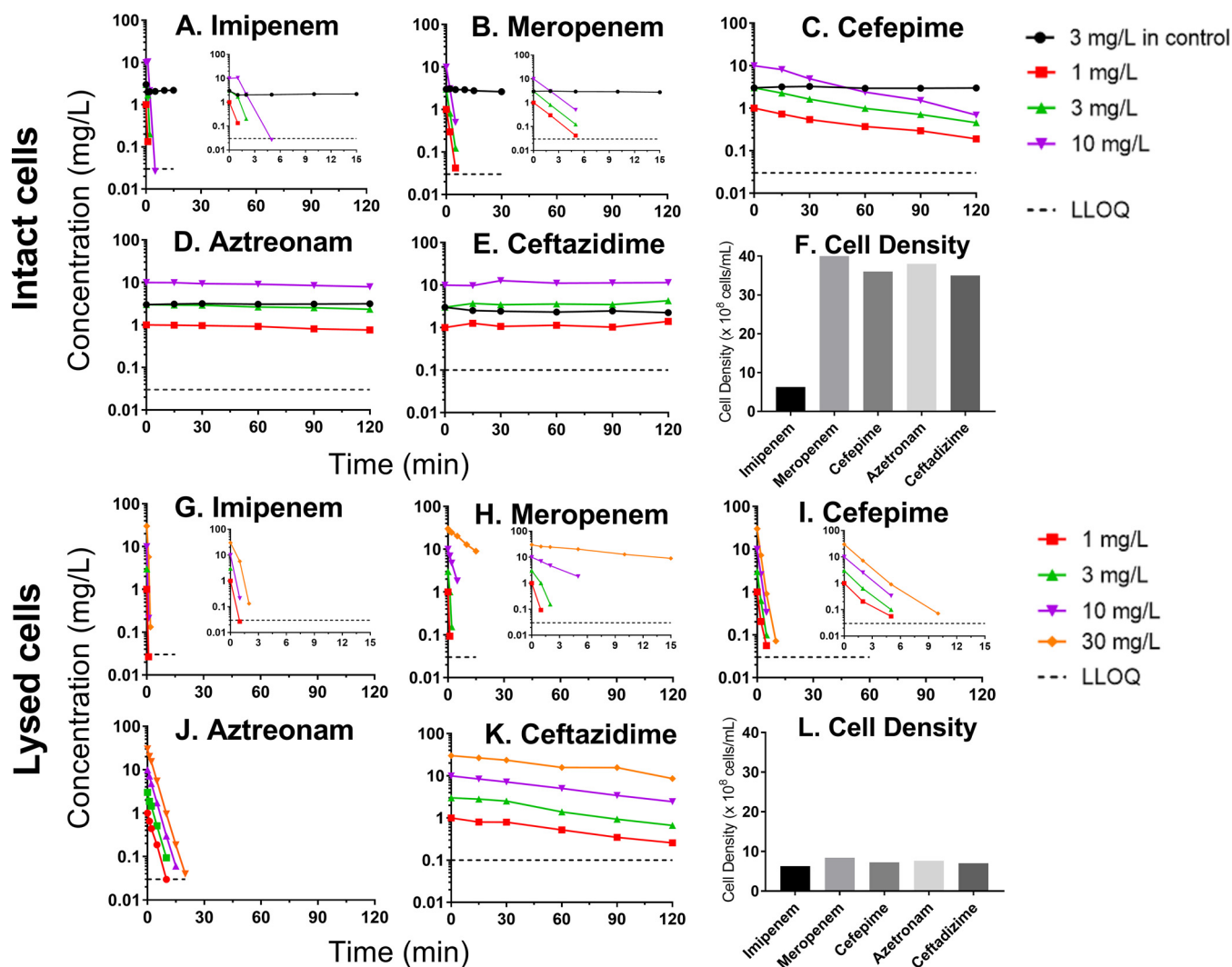
FIG 3 Concentration-time profiles of imipenem, meropenem, cefepime, ceftazidime, and aztreonam for the discrete assay of the polymyxin-susceptible *E. cloacae* isolate EC3800. β-Lactams were dosed at 3 mg/liter of each drug for the supernatant control and at 1, 3, or 10 mg/liter of each drug for intact bacteria arms (A to E). (F) Bacterial density (6.3×10^8 for imipenem, 4.2×10^9 for meropenem, 3.6×10^9 for cefepime, 3.8×10^9 for aztreonam, and 3.5×10^9 for ceftazidime) after six washes and immediately before adding the antibiotic to the intact bacteria arms. β-Lactams were dosed at 1, 3, 10, or 30 mg/liter of each drug for lysed bacteria arms (G to K). (L) Bacterial density (6.3×10^8 for imipenem, 8.4×10^8 for meropenem, 7.2×10^8 for cefepime, 7.6×10^8 for aztreonam, and 7.0×10^8 for ceftazidime) after the washes and immediately before lysing. The data (Table 1) represent biological triplicates. The individual profiles for all replicates are presented in the supplemental material.

Meropenem degradation was fast, but ~7-fold slower than that of imipenem in EC3800 (Fig. 1 and 3, panels B); meropenem degradation was slower for intact KP3800 (Fig. 2 and 4, panels B) relative to that of EC3800. Of note, while the downslope of imipenem and meropenem was roughly comparable for the discrete assay (Fig. 3A and B, Fig. 4A and B), the bacterial density used for imipenem was considerably smaller than that used for meropenem studies (Fig. 3F and 4F). Therefore, imipenem penetrated the OM substantially faster than meropenem.

Compared to imipenem, the rate of depletion was 258-fold slower for cefepime and at least 2,000-fold slower for aztreonam. For intact EC3800 after 120 min of incubation, the remaining β-lactam concentration was approximately 30% for cefepime and 60% for aztreonam each compared to their initial concentrations at time zero (Fig. 1 and 3, C and D). The depletion rates of the non-carbapenem β-lactams were even slower for intact KP3800 (Fig. 2 and 4, panels C and D). Finally, the rate of ceftazidime degradation was too slow to be robustly characterized (Fig. 1 to 4, panels E). The additional replicates of the cassette (Fig. S2 and S3) and discrete assay (Fig. S4 and S5) revealed
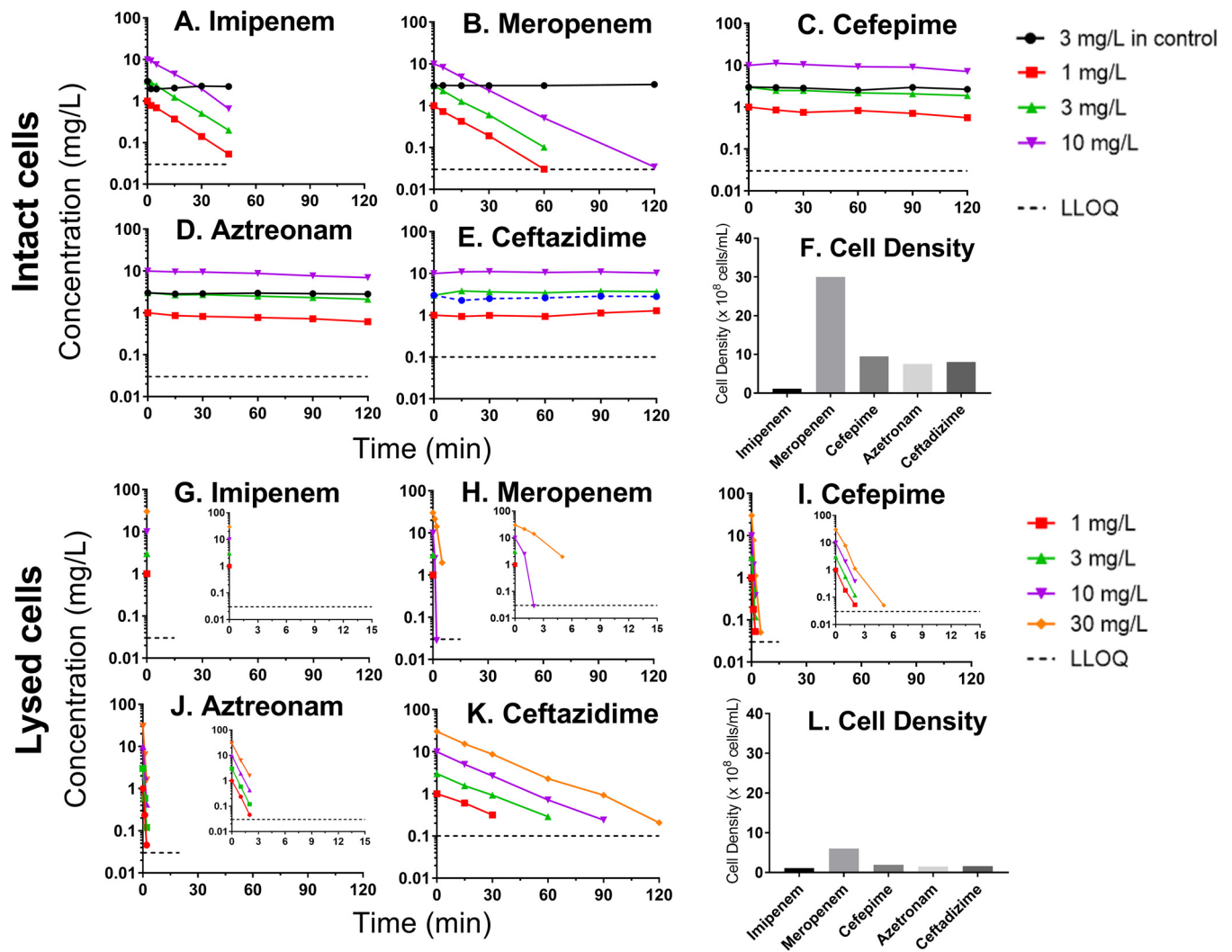
FIG 4 Concentration-time profiles of imipenem, meropenem, cefepime, ceftazidime, and aztreonam for the discrete assay of the polymyxin-resistant *K. pneumoniae* isolate KP3800. β-Lactams were dosed at 3 mg/liter each drug for the supernatant control and at 1, 3, or 10 mg/liter each drug for intact bacteria arms (A to E). (F) Bacterial density (1.1×10^8 for imipenem, 3.0×10^9 for meropenem, 9.5×10^8 for cefepime, 7.8×10^8 for aztreonam, and 7.5×10^8 for ceftazidime) after six washes and immediately before adding the antibiotic to the intact bacteria arms. β-Lactams were dosed at 1, 3, 10, or 30 mg/liter each drug for lysed cells arms (G to K). (L) Bacterial density (1.1×10^8 for imipenem, 6.0×10^8 for meropenem, 1.9×10^8 for cefepime, 1.5×10^8 for aztreonam, and 1.6×10^8 for ceftazidime) after the washes and immediately before lysing. The data (Table 1) represent biological triplicates. The individual profiles for all replicates are presented in the supplemental material.

good reproducibility compared to the first replicate (Fig. 1 to 4). Furthermore, we utilized the efflux pump inhibitor phenylalanine-arginine β-naphthylamide (PAβN) at 25 mg/liter and then carried out the cassette assay in intact bacteria. The depletion rates of all five β-lactams with PAβN coincubation (Fig. S6 and S7) were compared to assays without PAβN (Fig. 1 to 4 and Fig. S2 to S3).

Determination of OM permeability. After effective removal of extracellular β-lactamase by six washes, the depletion of β-lactam concentrations using intact bacteria can be attributed to periplasmic β-lactamase activity. For this scenario, penetration of β-lactam molecules through the OM presents the rate-limiting step and the decline of extracellular β-lactam concentrations is permeability limited. To characterize the time course of β-lactam degradation, we developed a mathematical model which included a distribution clearance (CLd) between the extracellular and periplasmic space. The CLd was independently estimated based on three biological replicates for the cassette assay and three biological replicates for the discrete assay. To convert the estimated CLd to permeability coefficients, the bacterial cell surface area and the initial

TABLE 1 Outer membrane permeability coefficients for imipenem, meropenem, cefepime, aztreonam and ceftazidime for the polymyxin-susceptible *E. cloacae* (EC3800) and the polymyxin-resistant *K. pneumoniae* (KP3800) isolates[a]

Assay and colony	Avg OM permeability coefficient (nm/s) ± SD				
	Imipenem	Meropenem	Cefepime	Aztreonam	Ceftazidime
Discrete *E. cloacae*	6,655 ± 2,542	729 ± 155	25.8 ± 15.2	1.34 ± 1.19	NA
Cassette *E. cloacae*	5,770 ± 1,570	843 ± 292	11.8 ± 4.45	3.20 ± 0.987	NA
Cassette *E. cloacae*, efflux	3,930 ± 920	402 ± 69.8	12.1 ± 4.26	5.10 ± 0.242	NA
Discrete *K. pneumoniae*	2,042 ± 338	83.3 ± 9.17	13.6 ± 9.26	8.64 ± 8.46	TSTD
Cassette *K. pneumoniae*	907 ± 65.7	90.7 ± 6.89	TSTD	TSTD	TSTD
Cassette *K. pneumoniae*, efflux	723 ± 124	57.5 ± 21.7	TSTD	TSTD	TSTD

[a]Data were determined via a discrete and a cassette assay, and additional cassette assay ("efflux") studies were carried out with 25 mg/liter phenylalanine-arginine β-naphthylamide (PAβN) as an efflux pump inhibitor. Estimates represent averages from three biological replicates for the cassette and discrete assays and two biological replicates for efflux inhibitor assay. TSTD, too slow to be determined (for the initial inocula used; TSTD is equivalent to a permeability coefficient of <0.6 nm/s for the experiments with *E. cloacae* isolate and <3 nm/s for the *K. pneumoniae* isolate); NA, not quantifiable in this isolate due to insufficient hydrolysis of ceftazidime.

inoculum used in the respective experiment were utilized. Lakaye et al. (24) published a conversion factor of 132 cm²/1 mg (dry weight) of cells, and one cell contributed 0.28 pg (dry weight) (25). This yields a bacterial surface area of 24.4 cm²/ml for an average initial inoculum of 6.6×10^8 CFU/ml for EC3800, equivalent to 3.7 μm² per cell.

Based on this conversion factor and the employed initial inocula, imipenem permeability was ~7-fold faster than that of meropenem, 258-fold faster than that of cefepime, and ~2,000-fold faster than that of aztreonam for EC3800 (Table 1). The permeability coefficient for ceftazidime could not be determined for EC3800 due to limited β-lactamase-mediated hydrolysis of ceftazidime (Fig. 1 and 3, panels E).

When comparing KP3800 to EC3800, the OM permeability coefficients were approximately 5-fold smaller for imipenem, 10-fold smaller for meropenem, and 3-fold smaller for cefepime in KP3800; however, the permeability coefficient was ~6-fold larger for aztreonam in KP3800. For ceftazidime, the KP3800 isolate displayed more β-lactamase-mediated hydrolysis than EC3800. However, degradation of ceftazidime was too slow to be reliably determined in intact bacteria. Given this, the permeability coefficient of ceftazidime was small (likely <3 nm/s) in KP3800. Addition of the efflux pump inhibitor PAβN at 25 mg/liter yielded similar OM permeability coefficients compared to the cassette assay without efflux pump inhibitor. The OM permeability coefficients were slightly smaller for the carbapenems and slightly larger for cefepime and aztreonam, but none of these comparisons with or without PAβN was statistically significant ($P >$ 0.05, unpaired t test).

To further assess the robustness of this assay, we ran a single replicate for two additional *K. pneumoniae* isolates (KP6478 and KP6484) using the discrete assay. Although some strain-to-strain variability in the OM permeability was observed (Table S2), the results were consistent with those for isolate KP3800, and the ranking of compounds was the same in all three isolates. The only exception was a faster OM permeability of ceftazidime in one of the three *K. pneumoniae* strains.

Proteomics and gene expression. To characterize the OM and efflux pump profiles, we used nano-LC/MS/MS to identify three OM porins, one β-lactamase and two efflux pump components. To confirm that the differences in protein expression were related to changes in mRNA expression, we performed reverse transcription-quantitative PCR (RT-qPCR) for selected genes (Fig. S8). Proteomics studies assessed the production of the OM porins OmpA, OmpK36/OmpC, and LamB; the KPC-2 β-lactamase; and the AcrB and TolC efflux pump components. When KP3800 and EC3800 were compared to *K. pneumoniae* strain ATCC 13833, OmpK36 was considerably more abundant in the ATCC strain (Table 2). Moreover, OmpC was more abundant in EC3800 than OmpK36 in KP3800. This correlated with the faster OM permeability in EC3800 compared to that in KP3800. In agreement with a prior publication showing a lack of OmpK35 in the ATCC strain (26, 27), we did not find this porin in either the ATCC strain or in our clinical isolates. The KPC-2 carbapenemase was the predominant β-lactamase in our clinical isolates and was produced in even higher abundance in KP3800 than in

TABLE 2 Protein production in strain ATCC 13833, a polymyxin-resistant *K. pneumoniae* isolate (KP3800), and a polymyxin-susceptible *E. cloacae* isolate (EC3800)

Protein	Protein production (normalized total spectra)		
	K. pneumoniae ATCC 13833	*K. pneumoniae* KP3800	*E. cloacae* (EC3800)
OmpA	170	237	90.0
OmpK35/OmpF	0.00	0.00	0.00
OmpK36/OmpC	36.0	9.00	18.0
LamB	81.0	46.0	24.0
KPC-2	0.00	12.0	3.00
AcrB	9.00	9.00	9.00
TolC	9.00	9.00	9.00

EC3800 (Table 2). This agreed with the substantially faster hydrolysis rate in lysed KP3800 compared to that of lysed EC3800.

DISCUSSION

This study developed a new, efficient OM permeability assay that can simultaneously quantify the permeability coefficients of five clinically relevant β-lactams. This assay has been optimized to assess OM permeability in MDR clinical isolates of *K. pneumoniae* and *E. cloacae* and should be applicable to a range of other isolates with different β-lactamases. Adapting this assay to a larger range of strains for the two tested pathogens should be reasonably readily achievable based on the detailed methods described here; implementing this assay in cassette mode will greatly benefit from support by a bioanalytical LC-MS/MS team. Expanding this assay to other pathogens may require further, pathogen-specific optimization.

In our isolates, there was no drug-drug interaction during influx for drug concentrations of up to 10 mg/liter for all five β-lactams simultaneously, as shown by the similar OM permeability coefficients obtained via the discrete and cassette assay. Consistent between the cassette and discrete assay, imipenem penetrated the OM of EC3800 approximately 7-fold faster than meropenem, 258-fold faster than cefepime, and 2,000-fold faster than aztreonam. Ceftazidime hydrolysis was very limited in EC3800 and moderate in KP3800, as expected based on prior reports on KPC-2 (28, 29); therefore, OM permeability estimates for ceftazidime carried more uncertainty, especially for EC3800.

The faster penetration of imipenem compared to meropenem in EC3800 was much more pronounced than the previously reported 2.74-fold faster OM permeability for imipenem over meropenem in *P. aeruginosa* (8). The permeability coefficient for cefepime in EC3800 was in the range of permeability coefficients (9.2 to 29 nm/s) reported previously for *E. cloacae* complex (9, 30, 31). Likewise, one prior study (30) reported permeability coefficients of 1 nm/s for ceftazidime and another study found an extremely low permeability coefficient of 0.032 nm/s for aztreonam (24).

The permeability coefficients were approximately 5- to 10-fold slower for KP3800 compared to those for EC3800, depending on the β-lactam. We are not aware of published permeability data for carbapenems in *E. cloacae* complex or *K. pneumoniae* (32). To the best of our knowledge, this is the first report showing a substantially faster OM penetration of carbapenems (especially imipenem) compared to the studied noncarbapenem β-lactams in *K. pneumoniae* and *E. cloacae*. Although considerably more work is required to prove the following hypothesis, the substantially faster OM permeability of imipenem compared to that of meropenem might be explained as follows. Imipenem has a leaner side chain than meropenem. Meropenem carries the positive charge on the nitrogen of a five-ring heterocycle (pKa$_2$ = 8.3); in contrast, imipenem is a stronger base (pKa$_2$ = 10.6) and the charge is located on a more flexible linear side chain at the R3 position. Moreover, imipenem lacks the methyl-group which is present in meropenem at the R2 position of the carbapenem backbone structure. These features might allow imipenem to align its negative and more defined positive

charges more efficiently while passing through OM porin channels. Future structural biology and computational chemistry work is warranted.

The vast majority of earlier studies used spectrophotometric methods with UV absorption to quantify β-lactam concentrations (7). The proposed new cassette assay offers several advantages. The LC-MS/MS assay we used has greatly improved selectivity and sensitivity compared to spectrophotometric methods. This allowed us to employ the LC-MS/MS assay in cassette and discrete modes and to demonstrate a lack of influx-related drug-drug interactions for the five β-lactams. Therefore, this assay enables characterization of the rate of OM permeability of double β-lactam combinations (12). The ranking of OM permeability coefficients matched between the discrete and cassette assay, and the results were comparable (Table 1). The cassette assay allowed us to better standardize the initial inoculum when comparing different β-lactams, since the same batch of bacteria is used to hydrolyze each β-lactam. In addition, the cassette assay provides improved efficiency for future studies in a larger number of strains (Table S2). The discrete assay offers the advantage that it completely avoids potential drug-drug interactions at any stage and that the bacterial density can be fine-tuned according to the rate of OM permeability (i.e., low bacterial density for rapidly penetrating drugs and vice versa). This improves the dynamic range of the assay. Importantly, both versions of this assay directly characterize OM permeability in MDR clinical isolates of $K.$ $pneumoniae$ and $E.$ $cloacae$ and do not rely on model systems. Employing both the discrete and the cassette versions of this assay allowed us to show a lack of impact of drug-drug interactions relating to influx, efflux, and β-lactamase activity. Therefore, combining both assay variants offers additional insights.

Our OM permeability data show a much faster penetration for EC3800 compared to that of KP3800. Proteomics confirmed this finding by revealing a lower production of the OmpK36 porin in KP3800 compared to the production of OmpC in EC3800 (Table 2). Likewise, production of the KPC-2 β-lactamase was 3-fold higher in KP3800, which correlated with the observed rate of hydrolysis in lysed bacteria (Fig. 1 to 4). The greatly decreased OM permeability and the increased KPC-2 β-lactamase production in KP3800 compared to those in EC3800 make the former isolate extensively more difficult to kill by β-lactam antibiotics, in agreement with the observed MICs. This demonstrates that the combination of our new OM permeability assay, whole-genome sequencing, and proteomics can provide mechanistic insights, which will be important for the future design of efficacious combination dosing strategies.

Two major OM porins, OmpK35 and OmpK36, have been identified in $K.$ $pneumoniae$ and shown to be relevant for β-lactam penetration. Lack of production of either or both of these porins has been shown to increase the MIC to certain β-lactams (33). When the large-diameter porins OmpK35 and OmpK36 are not produced, some data suggest that a normally quiescent porin, OmpK37, may contribute to the OM penetration of carbapenems (33). For $E.$ $cloacae$, outer membrane porins OmpF and OmpC have been identified and are involved in OM penetration (4). This may have contributed to the faster OM permeability for β-lactams in EC3800 (Table 2). Of note, we did not find differences in the production of the AcrB and TolC efflux pump components between either of our isolates or the ATCC strain. The presence or absence of the efflux pump inhibitor PAβN did not significantly affect the OM permeability estimates of our β-lactams in EC3800 and KP3800. This suggested that efflux did not affect the OM permeability results in the tested strains.

These mechanistic insights provide a foundation to inform efficacious antibiotic (combination) dosing strategies, which hold promise to combat MDR $K.$ $pneumoniae$ and $E.$ $cloacae$. Double β-lactam combination therapy has shown promising efficacy in early clinical trials for patients with infections by susceptible $Klebsiella$ spp. (12, 34, 35); this topic has received increasing attention. When each β-lactam inactivates its highest affinity PBP target, double β-lactam combination therapy offers the potential to inactivate an optimal set of PBPs. The present work revealed dramatic differences in the rate of OM penetration, which likely affect the time course of PBP inactivation. Moreover, the new cassette assay allowed us to demonstrate the absence of a drug-drug

interaction during influx when five β-lactams were used simultaneously at clinically relevant concentrations (Table 1 and Table S1). This supports the use of double β-lactam combinations in *K. pneumoniae* and suggests further *in vitro* studies for *E. cloacae*. Future studies are also warranted to assess potential influx-related interactions between β-lactams and β-lactamase inhibitors.

In conclusion, we developed and validated here a novel LC-MS/MS-based assay that can quantify the OM permeability of five β-lactams simultaneously for MDR *K. pneumoniae* and *E. cloacae*. Imipenem penetrated the OM at least 197-fold faster than the tested noncarbapenem β-lactams in our *E. cloacae* isolate and at least 118-fold faster in our *K. pneumoniae* isolate. Of note, imipenem penetrated substantially faster than meropenem. These findings were consistent between both isolates and between the cassette and discrete assay. The OM permeability was substantially slower and the β-lactamase production considerably greater in our *K. pneumoniae* isolate. Combined with supportive whole-genome sequencing and proteomics data, this new assay efficiently ranked the OM permeabilities of different clinically relevant β-lactams in our MDR clinical isolates. Overall, these new insights hold excellent promise to significantly enhance our mechanistic understanding of target site penetration, the rate of receptor binding and subsequent bacterial killing for combating MDR Gram-negative strains.

MATERIALS AND METHODS

Bacterial strains and reagents. One carbapenem-resistant clinical isolate each of *K. pneumoniae* (KP3800) and *E. cloacae* (EC3800) were used for all OM permeability studies. Two additional *K. pneumoniae* isolates (KP6478 and KP6484) were used for additional OM permeability studies to further support the developed assay and obtain insights on strain-to-strain variability. Imipenem and meropenem were purchased from AK Scientific (Union City, CA). Ceftazidime, cefepime, aztreonam, and PAβN were obtained from Chem-Impex International (Wood Dale, IL). Water and methanol (both LC-MS grade) were purchased from Fisher Scientific (Fair Lawn, NJ). Formic acid was acquired from Sigma-Aldrich (St. Louis, MO). Bacteria were grown in cation-adjusted Mueller-Hinton broth (MHII; BD BBL, Sparks, MD), and agar MICs (14) were determined according to CLSI guidelines (14, 36).

To predict the clinically relevant range of β-lactam concentrations, we performed Monte Carlo simulations to calculate the average unbound concentration at steady state in critically ill patients at the highest clinical dose (5). These simulations were performed for a continuous infusion and based on a literature review for the pharmacokinetics of each compound (imipenem [37–40], meropenem [41–45], cefepime [46], ceftazidime [47, 48], and aztreonam [38, 49]).

Supernatant control, intact, and lysed cell preparation. Bacteria (i.e., one colony) were grown in 50 ml of MHII broth for 4 h at 37°C. During this time, isolate EC3800 reached a density of approximately 6.0×10^8 CFU/ml and KP3800 of approximately 1.5×10^8 CFU/ml. These bacteria were in mid- (to late-) exponential growth phase. Bacteria were centrifuged at $4,750 \times g$ for 5 min, the supernatant was carefully discarded, and the bacterial pellet was resuspended in 50 ml of 50 mM potassium phosphate buffer at pH 7.0 containing 5 mM MgCl$_2$ following prior studies (50). This washing process was repeated six times. After the last wash, viable counts of the resuspended bacteria were determined. One part of the bacterial suspension was lysed by ultrasonication, and the other part was concentrated 5-fold to form the intact bacteria group. Due to rapid penetration of imipenem, this bacterial concentration step was not performed for the discrete assay of imipenem.

To evaluate the remaining β-lactamase activity after the washing steps, the supernatant of the washed and 5-fold concentrated bacterial suspension was carefully obtained at 0 h ("prior assay controls"). To additionally assess the extent of potential release of β-lactamase enzymes into the medium, the washed and 5-fold-concentrated bacterial suspension was further incubated for 2 h in PBS ("post assay controls"). For both the prior and post assay controls, the supernatant was obtained via centrifugation and used to quantify extracellular β-lactamase activity.

OM permeability assay. For the cassette assay, imipenem, meropenem, ceftazidime, cefepime, and aztreonam were added simultaneously, each at a concentration of 1, 3, or 10 mg/liter to the three intact bacteria arms (i.e., each arm used the same concentration of the five antibiotics). For the four lysed bacteria arms, 1, 3, 10, or 30 mg/liter of each β-lactam were used; the prior and post assay supernatant controls were spiked with 3 mg/liter of each β-lactam. The same range of drug concentrations was used for the discrete drug assay. Serial samples for LC-MS/MS analysis of antibiotic concentrations in PBS over time were collected up to 120 min post-dosing.

To investigate a potential contribution of efflux on the estimated OM permeability coefficients, additional cassette assay studies were performed using intact and lysed bacteria coincubated with the efflux pump inhibitor PAβN at 25 mg/liter; this concentration was chosen based on a prior study (51). The OM permeability coefficients in presence and absence of PAβN was compared for each β-lactam.

To further assess the robustness of the assay, OM permeability studies were performed in two additional *K. pneumoniae* isolates (KP6478 and KP6484) via the discrete assay. These results also provided first insights on strain-to-strain variability.

LC-MS/MS analysis. Imipenem, meropenem, ceftazidime, cefepime, and aztreonam were quantified by using LC-MS/MS. Our system consisted of a 1260 HPLC (Agilent) and a 6460 triple quadrupole mass spectrometer (Agilent). Separation was achieved using a Kinetex 2.6 μm Polar C$_{18}$ LC column (50 × 2.1 mm) with a run time of 7.0 min. Mobile phases consisted of 0.1% formic acid in water (phase A) and methanol (phase B) at a flow rate of 0.4 ml/min in gradient mode. The mass transition (MRM) of imipenem m/z 300.1 → 142.1, cefepime m/z 481.1 → 396.0, meropenem m/z 384.2 → 141.1, ceftazidime m/z 547.1 → 468.0, aztreonam 436.1 → 313.1, and the internal standard (diphenpydramine) m/z 256.2 → 167.2 were monitored in positive-ion mode.

Whole-genome sequencing. Genomic DNA was isolated using a DNeasy Blood and Tissue kit according to the "purification of total DNA from animal tissues" and "pretreatment for gram-negative bacteria pretreatment" protocols. Genomic DNA was quantified using the Quant-iT RiboGreen assay (Life Technologies.) Libraries were prepared from 1 ng of gDNA using a Nextera XT DNA Library Prep kit, and paired-end 250 cycle sequencing was performed on a MiSeq sequencer (Illumina). Genomes were assembled with the CLC Genomic Workbench and assemblies submitted to CGE MLST, ResFinder (52), and the CARD (53) servers for strain typing and resistance genotyping.

Analysis of gene expression. The relative mRNA levels of selected genes (*OmpK35/OmpF*, *OmpK36/OmpC*, *acrB*, *bla*$_{KPC-2}$ and *mgrB*) were determined by real-time RT-qPCR according to previously described protocols (54, 55). Total RNA was obtained with the RNeasy minikit (Qiagen). Fifty nanograms of purified RNA was used for one-step reverse transcription and real-time quantitative PCR run in ViiA 7 real-time PCR system usinga Power SYBR green RNA-to-CT 1-Step kit (Thermo Fisher). The 16S rRNA housekeeping gene *rrsE* was used to normalize the expression levels, and the results were referred to *K. pneumoniae* ATCC 13833 or EC3800. All RT-PCRs were performed in duplicate, and the mean values of expression from six independent experiments were considered. The primers used are listed in Fig. S8 in the supplemental material.

Proteomics and MS analysis. Nano-liquid chromatography-tandem mass spectrometry (Nano-LC-MS/MS) was performed on a Thermo Scientific Q Exactive HF Orbitrap mass spectrometer. The instrument was equipped with an EASY spray nanospray source (Thermo Fisher Scientific, San Jose, CA) and operated in positive-ion mode. An EASY Spray PepMAP column (Thermo Fisher) was used for chromatographic separations (C$_{18}$, 75 μm [inner diameter], 25-cm length, 3 μm, 100-Å pore size).

The scan sequence of the mass spectrometer was based on the TopFive method; analyses were programmed for a full scan recorded from 350 to 2,000 Da, and an MS/MS scan was used to generate product ion spectra. This approach determines the amino acid sequence in consecutive instrument scans for the ten most abundant peaks.

For database searching, all MS/MS samples were analyzed using the Sequest (XCorr Only; Thermo Fisher Scientific, San Jose, CA; version IseNode in Proteome Discoverer 2.2.0.388). Charge state deconvolution and deisotoping were not performed. Sequest (XCorr Only) was set up to search the Swiss-Prot database (version 2017_06; containing 554,860 sequences and 198,649,153 residues) using trypsin as digestion enzyme. Sequest (XCorr Only) was searched with a fragment ion mass tolerance of 0.020 Da and a parent ion tolerance of 10.0 ppm. Carbamidomethyl of cysteine was specified in Sequest (XCorr Only) as a fixed modification. Deamidation of asparagine and oxidation of methionine were specified in Sequest (XCorr Only) as variable modifications.

As criteria for protein identification, the Scaffold package (Scaffold_4.8.7; Proteome Software Inc., Portland, OR) was used to validate MS/MS-based peptide and protein identifications. Peptide identifications were accepted if they could be established at >95.0% probability by the Peptide Prophet algorithm (56) with the Scaffold delta-mass correction. Protein identifications were accepted if they could be established at >99.0% probability and contained at least one identified peptide. Protein probabilities were assigned by the Protein Prophet algorithm (57). Proteins which contained similar peptides and could not be differentiated based on MS/MS analysis alone were grouped to satisfy the principles of parsimony; likewise, proteins sharing significant peptide evidence were grouped into clusters.

Estimation of permeability coefficients. We developed a time course model to describe the drug concentrations in the extracellular and periplasmic space. This model included processes for β-lactam penetration from the extracellular into the periplasmic space, as well as β-lactamase-mediated hydrolysis of β-lactams in the periplasm of intact bacteria or in the extracellular space of lysed bacteria. As shown by the control arms, thermal degradation of the β-lactams was minimal over the 120-min study period. The supernatant control group was utilized to demonstrate the lack of any remaining extracellular β-lactamase activity after washing; the associated degradation clearance (CL$_{deg}$) was initially estimated and eventually fixed to zero. The differential equation for the amount of β-lactam (S) in the extracellular space of the control group was as follows:

$$\frac{dS}{dt} = -CL_{deg} \cdot S/V_S$$

The initial condition was set to 3 μg for S, and the supernatant volume (V$_S$) was fixed at 1 ml.

For intact bacteria, the distribution of β-lactams from the extracellular into periplasmic space was described by the distribution clearance (CLd). The potential degradation of extracellular β-lactam was described by CL$_{deg}$. In the periplasm, the β-lactamase mediated hydrolysis, followed Michaelis-Menten kinetics with a maximum rate of degradation (V_{max}) and a β-lactam concentration (K_m; Michaelis-Menten constant) associated with half-maximal V_{max}. The differential equations for the amounts of β-lactam in extracellular (E) and periplasmic (P) space were (C$_E$ and C$_P$ represent the β-lactam concentrations in the extracellular and periplasmic space):

$$C_E = E/V_E$$

$$C_P = P/V_P$$

$$\frac{dE}{dt} = -CF \cdot CLd \cdot C_E - CL_{deg} \cdot C_E + CF \cdot CLd \cdot C_P$$

$$\frac{dP}{dt} = CF \cdot CLd \cdot C_E - (CF \cdot V_{max} \cdot C_P)/(K_m + C_P) - CF \cdot CLd \cdot C_P$$

The concentration factor (CF) was introduced to account for the ~5-fold concentrated bacterial density of the intact bacteria group compared to that of the lysed group. The CF was 5 for all intact bacteria studies, except for the discrete studies with imipenem where CF was set to 1 (to reflect the experimental condition). The initial condition was set to 1, 3, or 10 μg for E and to 0 μg for P. Theoretically, the volume of 10^9 bacterial cells is only ~0.001 ml (and the periplasmic volume is a fraction of this). We confirmed during model building, that the chosen ratio of the periplasmic to the extracellular volume did not affect the CLd estimates, as long as the periplasmic volume was much smaller than the extracellular volume. We tested ratios of 5%, 1%, and 0.5% in our robust differential equation solver and confirmed this result via Laplace transformation (not shown). To enhance the stability of the differential equation solver (58), we fixed the periplasmic volume (V_P) to a value of 0.05 ml (which is considerably larger than the true biological volume [59]) and the extracellular volume (V_E) to 0.95 ml. This choice had minimal impact on the CLd estimates (CLd = distribution_rate_constant $\cdot$ V_E).

In lysed bacteria, β-lactams were freely exposed to β-lactamase enzymes. The hydrolysis followed the same Michaelis-Menten kinetics as in the aforementioned periplasmic compartment. A dilution factor of 20 was applied for V_{max}, to reflect the dilution of periplasmic content in the entire 1-ml volume after lysis (i.e., 0.05 ml versus 1 ml). The differential equation for the amount of drug in lysed bacteria arms (L) was (with C_L being the β-lactam concentration in the extracellular space):

$$C_L = L/V_L$$

$$\frac{dL}{dt} = -\frac{(V_{max}/20 \cdot C_L)}{(K_m + C_L)}$$

The initial conditions were set to 1, 3, 10, or 30 μg for L at time zero, and the lysed bacteria volume (V_L) was fixed to 1 ml.

To convert the estimated distribution clearance (CLd; unit, ml/min) to a permeability coefficient (nm/s), the bacterial surface area is needed. Lakaye et al. (24) published a conversion factor of 132 cm^2 per 1 mg (dry weight) of cells, and one cell contributed 0.28 pg (dry weight) (25). Therefore, one bacterial cell contributed a surface area of 3.7 μm^2. This estimate matched well with a previously published value (60). Consequently, for EC3800 6×10^8 cells were equivalent to a surface area of 22.2 cm^2, and for KP3800 1.5×10^8 cells were equivalent to 5.55 cm^2. The permeability coefficient (PC) was then calculated as follows:

$$PC \text{ (nm/s)} = \frac{CLd \cdot 10^7}{Surface\_area \cdot 60}$$

Estimation. To estimate the model parameters, we used the first-order conditional estimation method with the interaction option (FOCE+I) in the NONMEM software (version 7.4; ICON, Dublin, Ireland) (61). The Pirana facilitator tool was employed (62).

SUPPLEMENTAL MATERIAL

Supplemental material is available online only.

FIG S1, TIF file, 0.3 MB.
FIG S2, TIF file, 1.7 MB.
FIG S3, TIF file, 1.7 MB.
FIG S4, TIF file, 1.7 MB.
FIG S5, TIF file, 1.7 MB.
FIG S6, TIF file, 1.8 MB.
FIG S7, TIF file, 1.9 MB.
FIG S8, TIF file, 0.2 MB.
TABLE S1, DOCX file, 0.03 MB.
TABLE S2, DOCX file, 0.02 MB.

ACKNOWLEDGMENTS

REFERENCES

1. Munoz-Price LS, Poirel L, Bonomo RA, Schwaber MJ, Daikos GL, Cormican M, Cornaglia G, Garau J, Gniadkowski M, Hayden MK, Kumarasamy K, Livermore DM, Maya JJ, Nordmann P, Patel JB, Paterson DL, Pitout J, Villegas MV, Wang H, Woodford N, Quinn JP. 2013. Clinical epidemiology of the global expansion of *Klebsiella pneumoniae* carbapenemases. Lancet Infect Dis 13:785–796. https://doi.org/10.1016/S1473-3099(13)70190-7.

2. Nikaido H, Vaara M. 1985. Molecular basis of bacterial outer membrane permeability. Microbiol Rev 49:1–32.

3. Nikaido H. 2003. Molecular basis of bacterial outer membrane permeability revisited. Microbiol Mol Biol Rev 67:593–656. https://doi.org/10.1128/mmbr.67.4.593-656.2003.

4. Pages JM, James CE, Winterhalter M. 2008. The porin and the permeating antibiotic: a selective diffusion barrier in Gram-negative bacteria. Nat Rev Microbiol 6:893–903. https://doi.org/10.1038/nrmicro1994.

5. Bulitta JB, Landersdorfer CB, Forrest A, Brown SV, Neely MN, Tsuji BT, Louie A. 2011. Relevance of pharmacokinetic and pharmacodynamic modeling to clinical care of critically ill patients. Curr Pharm Biotechnol 12:2044–2061. https://doi.org/10.2174/138920111798808428.

6. Zavascki AP, Klee BO, Bulitta JB. 2017. Aminoglycosides against carbapenem-resistant *Enterobacteriaceae* in the critically ill: the pitfalls of aminoglycoside susceptibility. Expert Rev Anti-Infect Ther 15:519–526. https://doi.org/10.1080/14787210.2017.1316193.

7. Zimmermann W, Rosselet A. 1977. Function of the outer membrane of *Escherichia coli* as a permeability barrier to beta-lactam antibiotics. Antimicrob Agents Chemother 12:368–372. https://doi.org/10.1128/aac.12.3.368.

8. Iyobe S, Watanabe M, Mitsuhashi S, Inoue M. 1999. Estimation of outer membrane permeability of carbapenem antibiotics to *Pseudomonas aeruginosa*. J Infect Chemother 5:168–170. https://doi.org/10.1007/s101560050028.

9. Bellido F, Pechere JC, Hancock RE. 1991. Novel method for measurement of outer membrane permeability to new beta-lactams in intact *Enterobacter cloacae* cells. Antimicrob Agents Chemother 35:68–72. https://doi.org/10.1128/aac.35.1.68.

10. Mazzariol A, Cornaglia G, Nikaido H. 2000. Contributions of the AmpC beta-lactamase and the AcrAB multidrug efflux system in intrinsic resistance of *Escherichia coli* K-12 to beta-lactams. Antimicrob Agents Chemother 44:1387–1390. https://doi.org/10.1128/aac.44.5.1387-1390.2000.

11. Zapun A, Contreras-Martel C, Vernet T. 2008. Penicillin-binding proteins and β-lactam resistance. FEMS Microbiol Rev 32:361–385. https://doi.org/10.1111/j.1574-6976.2007.00095.x.

12. Jiao Y, Moya B, Chen MJ, Zavascki AP, Tsai H, Tao X, Sutaria DS, Louie A, Boyce JD, Deveson Lucas D, Kim TH, Tsuji BT, Bonomo RA, Drusano GL, Bulitta JB. 2019. Comparable efficacy and better safety of double beta-lactam combination therapy versus β-lactam plus aminoglycoside in Gram-negative bacteria in randomized controlled trials. Antimicrob Agents Chemother 63. https://doi.org/10.1128/AAC.00425-19.

13. Yadav R, Bulitta JB, Nation RL, Landersdorfer CB. 2016. Optimization of synergistic combination regimens against carbapenem- and aminoglycoside-resistant clinical *Pseudomonas aeruginosa* isolates via mechanism-based pharmacokinetic/pharmacodynamic modeling. Antimicrob Agents Chemother 61. https://doi.org/10.1128/AAC.01011-16.

14. Yadav R, Bulitta JB, Schneider EK, Shin BS, Velkov T, Nation RL, Landersdorfer CB. 2017. Aminoglycoside concentrations required for synergy with carbapenems against *Pseudomonas aeruginosa* determined via mechanistic studies and modeling. Antimicrob Agents Chemother 61: e00722-17. https://doi.org/10.1128/AAC.00722-17.

15. Vaara M. 1992. Agents that increase the permeability of the outer membrane. Microbiol Rev 56:395–411.

16. Savage PB. 2001. Multidrug-resistant bacteria: overcoming antibiotic permeability barriers of gram-negative bacteria. Ann Med 33:167–171. https://doi.org/10.3109/07853890109002073.

17. Yang CH, Glover KP, Han X. 2010. Characterization of cellular uptake of perfluorooctanoate via organic anion-transporting polypeptide 1A2, organic anion transporter 4, and urate transporter 1 for their potential roles in mediating human renal reabsorption of perfluorocarboxylates. Toxicol Sci 117:294–302. https://doi.org/10.1093/toxsci/kfq219.

18. Bosnar M, Kelnerić Z, Munić V, Eraković V, Parnham MJ. 2005. Cellular uptake and efflux of azithromycin, erythromycin, clarithromycin, telithromycin, and cethromycin. Antimicrob Agents Chemother 49: 2372–2377. https://doi.org/10.1128/AAC.49.6.2372-2377.2005.

19. Richter MF, Drown BS, Riley AP, Garcia A, Shirai T, Svec RL, Hergenrother PJ. 2017. Predictive compound accumulation rules yield a broad-spectrum antibiotic. Nature 545:299–304. https://doi.org/10.1038/nature22308.

20. Isabella VM, Campbell AJ, Manchester J, Sylvester M, Nayar AS, Ferguson KE, Tommasi R, Miller AA. 2015. Toward the rational design of carbapenem uptake in *Pseudomonas aeruginosa*. Chem Biol 22:535–547. https://doi.org/10.1016/j.chembiol.2015.03.018.

21. Zimmermann W. 1979. Penetration through the gram-negative cell wall: a co-determinant of the efficacy of beta-lactam antibiotics. Int J Clin Pharmacol Biopharm 17:131–134.

22. Di L, Keefer C, Scott DO, Strelevitz TJ, Chang G, Bi YA, Lai Y, Duckworth J, Fenner K, Troutman MD, Obach RS. 2012. Mechanistic insights from comparing intrinsic clearance values between human liver microsomes and hepatocytes to guide drug design. Eur J Med Chem 57:441–448. https://doi.org/10.1016/j.ejmech.2012.06.043.

23. Parker AJ, Houston JB. 2008. Rate-limiting steps in hepatic drug clearance: comparison of hepatocellular uptake and metabolism with microsomal metabolism of saquinavir, nelfinavir, and ritonavir. Drug Metab Dispos 36:1375–1384. https://doi.org/10.1124/dmd.108.020917.

24. Lakaye B, Dubus A, Joris B, Frere JM. 2002. Method for estimation of low outer membrane permeability to beta-lactam antibiotics. Antimicrob Agents Chemother 46:2901–2907. https://doi.org/10.1128/aac.46.9.2901-2907.2002.

25. Neidhardt FC. 1987. Escherichia coli and Salmonella Typhimurium: cellular and molecular biology. ASM Press, Washington, DC.

26. Tsai YK, Fung CP, Lin JC, Chen JH, Chang FY, Chen TL, Siu LK. 2011. *Klebsiella pneumoniae* outer membrane porins OmpK35 and OmpK36 play roles in both antimicrobial resistance and virulence. Antimicrob Agents Chemother 55:1485–1493. https://doi.org/10.1128/AAC.01275-10.

27. Hu YY, Cai JC, Zhou HW, Zhang R, Chen GX. 2015. Rapid detection of porins by matrix-assisted laser desorption/ionization-time of flight mass spectrometry. Front Microbiol 6:784. https://doi.org/10.3389/fmicb.2015.00784.

28. Mehta SC, Rice K, Palzkill T. 2015. Natural variants of the KPC-2 carbapenemase have evolved increased catalytic efficiency for ceftazidime hydrolysis at the cost of enzyme stability. PLoS Pathog 11:e1004949. https://doi.org/10.1371/journal.ppat.1004949.

29. Yigit H, Queenan AM, Anderson GJ, Domenech-Sanchez A, Biddle JW, Steward CD, Alberti S, Bush K, Tenover FC. 2001. Novel carbapenem-hydrolyzing β-lactamase, KPC-1, from a carbapenem-resistant strain of *Klebsiella pneumoniae*. Antimicrob Agents Chemother 45:1151–1161. https://doi.org/10.1128/AAC.45.4.1151-1161.2001.

30. Nikaido H, Liu W, Rosenberg EY. 1990. Outer membrane permeability

and beta-lactamase stability of dipolar ionic cephalosporins containing methoxyimino substituents. Antimicrob Agents Chemother 34:337–342. https://doi.org/10.1128/aac.34.2.337.

31. Hancock RE, Bellido F. 1992. Factors involved in the enhanced efficacy against gram-negative bacteria of fourth generation cephalosporins. J Antimicrob Chemother 29(Suppl A):1–6. https://doi.org/10.1093/jac/29.suppl_a.1.

32. Sugawara E, Kojima S, Nikaido H. 2016. *Klebsiella pneumoniae* major porins OmpK35 and OmpK36 allow more efficient diffusion of β-lactams than their *Escherichia coli* homologs OmpF and OmpC. J Bacteriol 198:3200–3208. https://doi.org/10.1128/JB.00590-16.

33. Delcour AH. 2009. Outer membrane permeability and antibiotic resistance. Biochim Biophys Acta 1794:808–816. https://doi.org/10.1016/j.bbapap.2008.11.005.

34. Spratt BG. 1983. Penicillin-binding proteins and the future of beta-lactam antibiotics: the seventh Fleming Lecture. J Gen Microbiol 129:1247–1260. https://doi.org/10.1099/00221287-129-5-1247.

35. Sutaria DS, Moya B, Green KB, Kim TH, Tao X, Jiao Y, Louie A, Drusano GL, Bulitta JB, Sutaria DS, Moya B, Green KB, Kim TH, Tao X, Jiao Y, Louie A, Drusano GL, Bulitta JB. 2018. First penicillin-binding protein occupancy patterns of β-lactams and β-lactamase inhibitors in *Klebsiella pneumoniae*. Antimicrob Agents Chemother 62. https://doi.org/10.1128/AAC.00282-18.

36. Clinical and Laboratory Standards Institute. 2015. Performance standards for antimicrobial susceptibility testing: 25th informational supplement. M100-S25. CLSI, Wayne, PA.

37. Dahyot C, Marchand S, Bodin M, Debeane B, Mimoz O, Couet W. 2008. Application of basic pharmacokinetic concepts to analysis of microdialysis data: illustration with imipenem muscle distribution. Clin Pharmacokinet 47:181–189. https://doi.org/10.2165/00003088-200847030-00004.

38. McKindley DS, Boucher BA, Hess MM, Croce MA, Fabian TC. 1996. Pharmacokinetics of aztreonam and imipenem in critically ill patients with pneumonia. Pharmacotherapy 16:924–931.

39. Lips M, Siller M, Strojil J, Urbanek K, Balik M, Suchankova H. 2014. Pharmacokinetics of imipenem in critically ill patients during empirical treatment of nosocomial pneumonia: a comparison of 0.5-h and 3-h infusions. Int J Antimicrob Agents 44:358–362. https://doi.org/10.1016/j.ijantimicag.2014.05.011.

40. Sakka SG, Glauner AK, Bulitta JB, Kinzig-Schippers M, Pfister W, Drusano GL, Sörgel F. 2007. Population pharmacokinetics and pharmacodynamics of continuous versus short-term infusion of imipenem-cilastatin in critically ill patients in a randomized, controlled trial. Antimicrob Agents Chemother 51:3304–3310. https://doi.org/10.1128/AAC.01318-06.

41. Thalhammer F, Traunmuller F, El Menyawi I, Frass M, Hollenstein UM, Locker GJ, Stoiser B, Staudinger T, Thalhammer-Scherrer R, Burgmann H. 1999. Continuous infusion versus intermittent administration of meropenem in critically ill patients. J Antimicrob Chemother 43:523–527. https://doi.org/10.1093/jac/43.4.523.

42. De Waele J, Carlier M, Hoste E, Depuydt P, Decruyenaere J, Wallis SC, Lipman J, Roberts JA. 2014. Extended versus bolus infusion of meropenem and piperacillin: a pharmacokinetic analysis. Minerva Anestesiol 80:1302–1309.

43. Roberts JA, Kirkpatrick CM, Roberts MS, Robertson TA, Dalley AJ, Lipman J. 2009. Meropenem dosing in critically ill patients with sepsis and without renal dysfunction: intermittent bolus versus continuous administration? Monte Carlo dosing simulations and subcutaneous tissue distribution. J Antimicrob Chemother 64:142–150. https://doi.org/10.1093/jac/dkp139.

44. Kitzes-Cohen R, Farin D, Piva G, De Myttenaere-Bursztein SA. 2002. Pharmacokinetics and pharmacodynamics of meropenem in critically ill patients. Int J Antimicrob Agents 19:105–110. https://doi.org/10.1016/S0924-8579(01)00474-5.

45. Adnan S, Li JX, Wallis SC, Rudd M, Jarrett P, Paterson DL, Lipman J, Udy AA, Roberts JA. 2013. Pharmacokinetics of meropenem and piperacillin

in critically ill patients with indwelling surgical drains. Int J Antimicrob Agents 42:90–93. https://doi.org/10.1016/j.ijantimicag.2013.02.023.

46. Lipman J, Wallis SC, Rickard C. 1999. Low plasma cefepime levels in critically ill septic patients: pharmacokinetic modeling indicates improved troughs with revised dosing. Antimicrob Agents Chemother 43:2559–2561. https://doi.org/10.1128/AAC.43.10.2559.

47. Hanes SD, Wood GC, Herring V, Croce MA, Fabian TC, Pritchard E, Boucher BA. 2000. Intermittent and continuous ceftazidime infusion for critically ill trauma patients. Am J Surg 179:436–440. https://doi.org/10.1016/s0002-9610(00)00388-3.

48. Young RJ, Lipman J, Gin T, Gomersall CD, Joynt GM, Oh TE. 1997. Intermittent bolus dosing of ceftazidime in critically ill patients. J Antimicrob Chemother 40:269–273. https://doi.org/10.1093/jac/40.2.269.

49. Ulldemolins M, Roberts JA, Rello J, Paterson DL, Lipman J. 2011. The effects of hypoalbuminaemia on optimizing antibacterial dosing in critically ill patients. Clin Pharmacokinet 50:99–110. https://doi.org/10.2165/11539220-000000000-00000.

50. Sugawara E, Nikaido H. 2012. OmpA is the principal nonspecific slow porin of *Acinetobacter baumannii*. J Bacteriol 194:4089–4096. https://doi.org/10.1128/JB.00435-12.

51. Lamers RP, Cavallari JF, Burrows LL. 2013. The efflux inhibitor phenylalanine-arginine beta-naphthylamide (PAβN) permeabilizes the outer membrane of gram-negative bacteria. PLoS One 8:e60666. https://doi.org/10.1371/journal.pone.0060666.

52. Zankari E, Hasman H, Cosentino S, Vestergaard M, Rasmussen S, Lund O, Aarestrup FM, Larsen MV. 2012. Identification of acquired antimicrobial resistance genes. J Antimicrob Chemother 67:2640–2644. https://doi.org/10.1093/jac/dks261.

53. Jia B, Raphenya AR, Alcock B, Waglechner N, Guo P, Tsang KK, Lago BA, Dave BM, Pereira S, Sharma AN, Doshi S, Courtot M, Lo R, Williams LE, Frye JG, Elsayegh T, Sardar D, Westman EL, Pawlowski AC, Johnson TA, Brinkman FS, Wright GD, McArthur AG. 2017. CARD 2017: expansion and model-centric curation of the comprehensive antibiotic resistance database. Nucleic Acids Res 45:D566–D573. https://doi.org/10.1093/nar/gkw1004.

54. Schmittgen TD, Livak KJ. 2008. Analyzing real-time PCR data by the comparative C_T method. Nat Protoc 3:1101–1108. https://doi.org/10.1038/nprot.2008.73.

55. Moya B, Dotsch A, Juan C, Blazquez J, Zamorano L, Haussler S, Oliver A. 2009. Beta-lactam resistance response triggered by inactivation of a nonessential penicillin-binding protein. PLoS Pathog 5:e1000353. https://doi.org/10.1371/journal.ppat.1000353.

56. Keller A, Nesvizhskii AI, Kolker E, Aebersold R. 2002. Empirical statistical model to estimate the accuracy of peptide identifications made by MS/MS and database search. Anal Chem 74:5383–5392. https://doi.org/10.1021/ac025747h.

57. Nesvizhskii AI, Keller A, Kolker E, Aebersold R. 2003. A statistical model for identifying proteins by tandem mass spectrometry. Anal Chem 75:4646–4658. https://doi.org/10.1021/ac0341261.

58. Materi W, Wishart DS. 2007. Computational systems biology in drug discovery and development: methods and applications. Drug Discov Today 12:295–303. https://doi.org/10.1016/j.drudis.2007.02.013.

59. Stock JB, Rauch B, Roseman S. 1977. Periplasmic space in Salmonella typhimurium and *Escherichia coli*. J Biol Chem 252:7850–7861.

60. Prats R, De Pedro M. 1989. Normal growth and division of *Escherichia coli* with a reduced amount of murein. J Bacteriol 171:3740–3745. https://doi.org/10.1128/jb.171.7.3740-3745.1989.

61. Bauer RJ, Guzy S, Ng C. 2007. A survey of population analysis methods and software for complex pharmacokinetic and pharmacodynamic models with examples. AAPS J 9:E60–E83. https://doi.org/10.1208/aapsj0901007.

62. Keizer RJ, Karlsson MO, Hooker A. 2013. Modeling and simulation workbench for NONMEM: tutorial on Pirana, PsN, and Xpose. CPT Pharmacometrics Syst Pharmacol 2:e50. https://doi.org/10.1038/psp.2013.24.